

1 **Abstract**

2 Recent studies have drawn attention to a significant weakening trend of the South Asian  
3 monsoon circulation and an associated decrease in regional rainfall during the last few  
4 decades. While surface temperatures over the region have steadily risen during this period,  
5 most of the CMIP (Coupled Model Intercomparison Project) global climate models have  
6 difficulties in capturing the observed decrease of monsoon precipitation, thus limiting our  
7 understanding of the regional land surface response to monsoonal changes. This problem is  
8 investigated by performing two long-term simulation experiments, with and without  
9 anthropogenic forcing, using a variable resolution global climate model having high-  
10 resolution zooming over the South Asian region. The present results indicate that  
11 anthropogenic effects have considerably influenced the recent weakening of the monsoon  
12 circulation and decline of precipitation. It is seen that the simulated increase of surface  
13 temperature over the Indian region during the post-1950s is accompanied by a significant  
14 decrease of monsoon precipitation and soil moisture. Our analysis further reveals that the  
15 land surface response to decrease of soil moisture is associated with significant reduction in  
16 evapotranspiration over the Indian land region. A future projection, based on the  
17 representative concentration pathway 4.5 (RCP4.5) scenario of the Intergovernmental panel  
18 on Climate Change (IPCC), using the same high-resolution model indicates the possibility for  
19 detecting the summer-time soil drying signal over the Indian region during the 21<sup>st</sup> century, in  
20 response to climate change. While these monsoon hydrological changes have profound socio-  
21 economic implications, the robustness of the high-resolution simulations provides deeper  
22 insights and enhances our understanding of the regional land surface response to the changing  
23 South Asian monsoon.

24

25 **1 Introduction**

26 The South Asian monsoon, also known as the Indian Summer Monsoon (ISM), brings  
27 approximately 70-80% of the annual rainfall of the region during the season June-September  
28 (JJAS) and is the major source for water needs of the densely populated country. Any  
29 changes in the South Asian monsoon rainfall (a component of the larger-scale Asian  
30 monsoon system) due to climate change will have serious impacts on the socio-economic  
31 conditions of the country. Understanding the monsoon hydroclimatic response to climate  
32 change is also of great scientific interest. Several recent studies have reported significant

1 negative trends in the observed seasonal monsoon precipitation on regional and sub-regional  
2 scales over South Asia since 1950s (e.g. Guhathakurta and Rajeevan 2006; Chung and  
3 Ramanathan, 2006; Bollasina et al., 2011; Krishnan et al., 2013; Rajendran et al., 2012; Saha  
4 et al., 2014; Singh et al., 2014 and others). Various studies have also noted a weakening trend  
5 of the large-scale summer monsoon circulation during recent decades (e.g. Tanaka et al.  
6 2004; Abish et al., 2013; Fan et al., 2010; Krishnan et al., 2013). Few modelling studies have  
7 attributed the climate forcing by aerosols as the major driver for the decreasing precipitation  
8 trend over the Indian region (see Chung and Ramanathan, 2006; Bollasina et al., 2011).  
9 There is also a view that rapid increase of moisture in a global warming environment can  
10 increase the atmospheric stability and weaken the tropical and monsoon circulations (e.g.  
11 Kitoh et al., 1997; Douville et al., 2000; Veechi et al., 2006; Ueda et al., 2006). High  
12 resolution model simulations reveal that a weakening of the southwesterly monsoon winds  
13 can in turn reduce orographic precipitation over the Western Ghat mountains (see Krishnan et  
14 al., 2013; Rajendran et al., 2012).

15 The satellite derived soil moisture data from the Tropical Rainfall Measuring Mission  
16 (TRMM) during 1998-2008 indicates significant decreasing trends in soil moisture and  
17 evapotranspiration over many places globally and also over the Indian region (Jung et al.,  
18 2010). An increasing trend in the intensity and percent area affected by moderate droughts  
19 over India is noted by Kumar et al. (2013) during recent decades using a drought monitoring  
20 index *viz.*, Standardized Precipitation Evapotranspiration Index (SPEI) which is based on  
21 climatic water balance. However, an understanding of whether these changes in soil moisture  
22 and evapotranspiration over India are responding to the anthropogenic forcing is lacking.  
23 This is in spite of the importance of these regional water balance components from scientific  
24 and societal perspectives, given their implications on climate, agriculture and other human  
25 activities (Seneviratne et al., 2006). One of the earliest investigations on the temporal and  
26 spatial variations of soil moisture response to global warming was conducted by Wetherald  
27 and Manabe (1999) using long-term integrations of a coupled atmosphere ocean global  
28 circulation model. Their results suggested that soil dryness due to global warming was  
29 prominently detectable over the mid-continental regions of middle and high latitudes by the  
30 first half of the 21<sup>st</sup> century. Over the Indian subcontinent, they noted an increase of soil  
31 moisture during the summer season due to increase of precipitation. However, these results  
32 were based on coarse resolution model simulations. Furthermore, models tend to exaggerate  
33 summer drying through overestimation of evaporation particularly in regions where soil

1 moisture and energy are not limited (Seneviratne et al., 2002). Proper understanding of land-  
2 surface response over the Indian region to climate change is lacking due to poor simulation of  
3 regional water balance in many coupled model intercomparison project (CMIP) models  
4 (Hasson et al., 2013). For example, Jourdain et al. (2013) reported a large spread in the  
5 simulated seasonal mean Indian summer monsoon rainfall as well as the seasonality of  
6 rainfall among the state-of-the-art CMIP5 coupled models used for the fifth Assessment  
7 Report of the Intergovernmental panel on Climate Change (IPCC). Also a majority of CMIP  
8 models do not adequately capture the historical trend of decreasing precipitation over Indian  
9 monsoon region (e.g. Saha et al., 2014), with large uncertainties in future projections in the  
10 magnitude of monsoon precipitation over the region (Chaturvedi et al., 2012).

11 In this study, we have used a variable resolution global climate model from Laboratoire de  
12 Météorologie Dynamique (LMD), France with high-resolution (grid size < 35 km) telescopic  
13 zooming over South Asia and includes a state-of-the-art land-surface model, to better  
14 understand the regional land surface hydrological response to monsoonal changes. The model  
15 simulations also account for transient changes in land-use and land-cover, which are  
16 prescribed from standard datasets used in the CMIP5 experiments (see next section). Sabin et  
17 al. (2013) have assessed the South Asian monsoon simulations from the telescopically  
18 zoomed LMD model. They noted that the high-resolution LMD simulations provide  
19 important value additions in representing moist convective processes and organized  
20 convective activity over the monsoon region; and also realistically captured the regional  
21 details of precipitation characteristics and their links to monsoonal circulation. This paper is  
22 organised as follows. Section 2 provides a description of the model, design of experiments  
23 and observed data used for this work. Results from the historical simulations and comparison  
24 with observations are discussed in Section 3. The results of land hydrological response are  
25 presented in Section 4. The detectable future changes in land hydrology are described in  
26 Section 5 and the conclusions are summarized in Section 6.

27

## 28 **2 Model, data and methods**

### 29 **2.1 Model and experiments**

30 The climate model used in this study is the LMD global atmospheric general circulation  
31 model (AGCM) with enhanced resolution capability over a particular region of interest (see

1 Hourdin et al., 2006; Sabin et al., 2013). The high resolution zoom used in the LMDZ ( where  
2 Z stands for zoom) model is centred at 15°N, 80°E. The zoom domain (15°S–40°N, 30°E–  
3 120°E) covers the entire South Asian monsoon region and the tropical Indian Ocean. The  
4 resolution is about 35 km in the zoom domain, and it becomes gradually coarser outside.  
5 Sabin et al. (2013) have evaluated different aspects of the South Asian monsoon simulation  
6 from this high-resolution model with telescopic zooming. The detailed description of the  
7 representation of physical processes in the version used here is given in Hourdin et al. (2006  
8 and the references therein).

9 The LMDZ AGCM and the state-of-the-art land surface model Organizing Carbon and  
10 Hydrology in Dynamic Ecosystems (ORCHIDEE; Krinner et al., 2005) are fully coupled with  
11 two way interactions between atmosphere and land surface. The ORCHIDEE includes the  
12 Schématisation des Echanges Hydriques à L’Interface Biosphère– Atmosphère surface-  
13 vegetation-atmosphere transfer scheme (SECHIBA; Ducoudré et al., 1993; de Rosnay and  
14 Polcher, 1998) and the Saclay Toulouse Orsay Model for the Analysis of Terrestrial  
15 Ecosystems carbon module (STOMATE). SECHIBA calculates the exchange of energy and  
16 water between the atmosphere and the biosphere along with the soil water budget.  
17 STOMATE simulates the phenology and carbon dynamics of the terrestrial biosphere such as  
18 photosynthesis, carbon allocation, litter decomposition, soil carbon dynamics, respiration etc.,  
19 ORCHIDEE builds on the concept of plant functional types (PFT) to describe vegetation  
20 distributions. The land surface is represented as a heterogeneous mosaic of 12 PFTs and bare  
21 soil. The PFTs are defined based on ecological parameters such as plant structure (tree or  
22 grass), leaves (needleleaf or broadleaf), phenology (evergreen, summergreen, or raingreen)  
23 and according to the type of photosynthesis for crops and grasses (C3 or C4).

24 We have conducted long-term simulation experiments using this configuration of the LMDZ  
25 GCM, with high-resolution (~ 35 km) zooming over South Asia. The first model simulation is  
26 the Historical run (HIST; 1886-2005), which uses both natural (e.g. Volcanoes and solar  
27 variability ) and anthropogenic (e.g. green house gases (GHG), aerosols evolution estimated  
28 from transport models, land use and land cover changes, etc) forcing. The second  
29 experiment is Historical Natural run (NAT; 1886 – 2005), which uses only natural (e.g.  
30 Volcanoes and solar variability) forcing. Another simulation, which is intended to understand  
31 likely future changes (2006 - 2095), uses both natural and anthropogenic forcing based on  
32 IPCC approved medium stabilization scenario Representative Concentration Pathway 4.5  
33 (RCP 4.5), in which the net radiative forcing at the end of 2100 is 4.5 Wm<sup>-2</sup>.

1 The monthly bias adjusted sea surface temperature (SST) and sea-ice from the CMIP5  
2 experiments with the coarser resolution atmosphere-ocean coupled GCM run from Institut  
3 Pierre Simon Laplace (IPSL-CM5A-LR; referred as IPSL hereafter) are used as boundary  
4 forcing for LMDZ experiments. Bias adjustment refers to the removal of model errors in  
5 present day mean climate. The SST anomalies for HIST, NAT and RCP4.5 experiments of  
6 IPSL are superposed on the observed climatological mean SST from the AMIP  
7 (Atmospheric Model Intercomparison Project) dataset ([http://www-](http://www-pcmdi.llnl.gov/projects/amip/AMIP2EXPDSN/BCS/amip2bcs.php)  
8 [pcmdi.llnl.gov/projects/amip/AMIP2EXPDSN/BCS/amip2bcs.php](http://www-pcmdi.llnl.gov/projects/amip/AMIP2EXPDSN/BCS/amip2bcs.php)). This methodology  
9 assumes the statistical stationarity hypothesis i.e., relationships inferred from historical data  
10 remain valid under a changing climate (Maraun 2012). The same procedure is applied for  
11 specifying sea-ice boundary conditions.

12 The land use changes are prescribed using the historical crop and pasture datasets developed  
13 by Hurtt et al. (2011), which are also being used for the IPCC CMIP5 simulations. These  
14 datasets provide information on human activities (crop land and grazed pastureland) on a  $0.5^\circ$   
15  $\times 0.5^\circ$  horizontal grid. The land-cover map used for both the historical and future period has  
16 been obtained starting from an observed present-day land-cover map (Loveland et al., 2000),  
17 which already includes both natural and anthropogenic vegetation types. These datasets are  
18 included in LMDZ following the methodology described by Dufresne et al. (2013).

## 19 **2.2 Data**

20 The model climate is compared with observational data to assess the model reliability. For  
21 this purpose we have used winds, precipitation and temperature data from observationally  
22 based and reanalysis estimates. The monthly circulation data at 850 hPa and 200 hPa is  
23 obtained from a recent reanalysis produced by the European Centre for Medium-Range  
24 Weather Forecasts (ECMWF) called ERA-Interim (ERA-Interim; Dee and Uppala, 2009; Dee et al.,  
25 2011) for the time period 1979-2005. Monthly Surface air temperature over land at the  $0.5^\circ \times$   
26  $0.5^\circ$  resolution from Climatic Research Unit (CRU TS3.1; Harris et al., 2014) for the period  
27 1951-2005 is used. Precipitation observations over land from the Asian Precipitation—  
28 Highly-Resolved Observational Data Integration Towards Evaluation of Water Resources  
29 (APHRODITE) gridded ( $0.5^\circ \times 0.5^\circ$ ) daily rainfall dataset (Yatagai et al. 2009) and from the  
30 India Meteorological Department (IMD) gridded ( $0.25^\circ \times 0.25^\circ$ ) daily rainfall dataset (Pai et  
31 al. 2014) for the period 1951-2005 are used. In order to compare the model simulated  
32 precipitation over ocean regions, the observational based monthly gridded ( $2.5^\circ \times 2.5^\circ$ )

1 precipitation data obtained from Climate Prediction Centre Merged Analysis of Precipitation  
2 (CMAP; Xie and Arkin, 1997) is also used. The model simulated monthly land surface  
3 hydrological components are compared with the corresponding multi-model mean computed  
4 from the multiple off-line land model simulations of Global Land Data Assimilation System  
5 (GLDAS; Rodell et al. 2004) available at 1°x 1° resolution.

## 6 **2.3 Methodology**

7 The long term mean summer monsoon climate simulated by the IPSL and LMDZ models are  
8 evaluated by comparing the spatial pattern of the wind circulation from their HIST  
9 simulations with the ERAI reanalysis. The spatial patterns of the simulated 2m temperature,  
10 precipitation and evapotranspiration for these model runs are also compared with the  
11 observational based gridded estimates. The pattern correlations for these model simulated  
12 fields are computed by regridding them on the corresponding reference data grid points to  
13 assess the ability of the IPSL and LMDZ models in capturing the large scale features of mean  
14 climate. Further the annual water balance in land region over India simulated in both the  
15 models is compared with the GLDAS estimates. The spatial patterns of the linear trends  
16 simulated by the IPSL and LMDZ models over India during the summer monsoon season for  
17 temperature and precipitation are evaluated by comparing with the CRU and APHRODITE  
18 gridded observational estimates respectively. The statistical significance of trends are tested  
19 using the Student t test. The LMDZ model simulated anthropogenic influence on the summer  
20 monsoon climate is assessed by comparing the area averaged linear trends of temperature and  
21 precipitation over Indian land region in the HIST with the NAT simulation of this model. The  
22 response of the land surface hydrology to anthropogenic forcing is brought out by computing  
23 the linear trends for total soil moisture and evapotranspiration for the historical as well as for  
24 a future climate change scenario. The detectability of soil moisture changes in response to the  
25 anthropogenic forcing is assessed following Wetherald and Manabe (1999), by comparing the  
26 magnitudes of soil moisture changes against the standard deviation of the natural soil  
27 moisture variability in the NAT integration. The soil moisture changes are computed with  
28 respect to the long term mean of NAT integration, and the changes are considered to be  
29 detectable when they exceed standard deviation of the natural variability.

## 30 **3 Model simulation of mean climate**

### 31 **3.1 Mean summer monsoon features**

1 In this section, the simulations of the mean summer monsoon in the LMDZ model and the  
2 driving IPSL model are discussed and validated by comparison with reanalysis products and  
3 gridded observational estimates. Figure 1 shows the JJAS mean climatology of the lower  
4 (850 hPa) and upper (200 hPa) tropospheric wind circulation. The large-scale low level  
5 circulation features viz., the cross equatorial monsoon flow across the Indian Ocean, the  
6 Somali jet over the Arabian Sea and the monsoon trough over the Indian subcontinent can be  
7 noted in ERAI, the IPSL and LMDZ simulations (Figs. 1a-c). The wind climatology along  
8 the monsoon trough and head Bay of Bengal simulated by LMDZ is relatively closer to  
9 ERAI, as compared to the IPSL simulation. The pattern correlation between the simulated  
10 and observed low level wind climatology over the domain (20°S-35°N, 40°E-120°E) is 0.93  
11 for LMDZ and 0.85 for the IPSL model. The major summer-time upper tropospheric wind  
12 circulation features such as the Tropical Easterly Jet over the Indian subcontinent, the Tibetan  
13 anticyclone and the subtropical westerly to the north of the subcontinent can be noted in  
14 ERAI and are captured in the IPSL and LMDZ simulations (Figs. 1d-f).

15 Figure 2 shows the spatial distributions of JJAS mean climatology of 2m air temperature,  
16 precipitation and evapotranspiration (ET). The region of high temperatures with east-west  
17 orientation over northwest India and Pakistan (Fig. 2a) coincides with the monsoon trough  
18 and is better captured in the high-resolution LMDZ simulation (Fig. 2c) as compared to the  
19 IPSL coarse resolution model (Fig. 2b). The near surface air temperatures are underestimated  
20 both in LMDZ and IPSL simulations over central and peninsular India. The pattern  
21 correlations of the simulated and observed (CRU) mean surface air temperature over the land  
22 region (70°-90°E, 10°-28°N) are found to be 0.95 and 0.81 for the LMDZ and IPSL models  
23 respectively.

24 We also compared the simulated mean precipitation from the LMDZ and IPSL models with  
25 the CMAP and APHRODITE precipitation datasets over the Indian monsoon region. The  
26 CMAP is a merged precipitation gridded product obtained by combining satellite and rain  
27 gauge observations and is available both over land and oceanic regions on a 2.5° x 2.5° grid  
28 (Xie and Arkin, 1997). The APHRODITE is a high resolution 0.5°x0.5° gridded rainfall  
29 dataset constructed from raingauge observations (Yatagai et al., 2012). The summer monsoon  
30 precipitation over central India and along the Indo Gangetic plains seen in the long term  
31 observed climatology from CMAP (Fig. 2d) are simulated relatively better in the LMDZ (Fig.  
32 2f) model than the driving IPSL model (Fig. 2e), even though their magnitudes over these

1 parts of India are lesser than the observed estimate. It is noted that LMDZ model is able to  
2 capture the rainfall peak over the Bay of Bengal (Fig. S1) and the area averaged rainfall over  
3 the region  $80^{\circ}$ - $98^{\circ}$  E;  $8^{\circ}$ - $22^{\circ}$  N covering Bay of Bengal is found to be  $10.54 \text{ mm d}^{-1}$  and  $8.48$   
4  $\text{mm d}^{-1}$  for CMAP and LMDZ respectively. It is also found that the high resolution LMDZ  
5 model simulated rainfall maxima along the west coast, foot hills of Himalayas and northeast  
6 India are closer to high resolution rain gauge based observed climatology from APHRODITE  
7 (see supplementary Fig. S2a). The pattern correlations of the simulated and observed  
8 (APHRODITE) mean precipitation over the Indian land region ( $70^{\circ}$ - $90^{\circ}$ E,  $10^{\circ}$ - $28^{\circ}$ N) are  
9 found to be 0.47 and 0.20 for the LMDZ and IPSL models respectively. Previous studies have  
10 shown that there is considerable spread among the different observed precipitation datasets  
11 over India (Collins et al. 2013; Kim et al. 2015). Our analysis using the  $0.25^{\circ} \times 0.25^{\circ}$  high-  
12 resolution rainfall dataset from IMD (Pai et al. 2014; Fig. S2b) shows that the area-averaged  
13 summer monsoon rainfall over India is comparable with the APHRODITE ( Fig. S3).

14 The simulated evapotranspiration (ET), which is a major component of hydrological cycle, is  
15 compared with the GLDAS gridded dataset (Rodell et al., 2004). Observational uncertainties  
16 of surface hydrologic variables are large (Bindoff et al., 2013). The GLDAS dataset integrates  
17 observation based data to drive multiple off-line land surface models to generate flux  
18 parameters and land surface state (e.g. soil moisture, evapotranspiration, runoff, sensible heat  
19 flux, etc). Since the GLDAS off-line land surface models are driven by observations and bias-  
20 corrected reanalysis fields, the multi-model estimates from GLDAS serve as physically  
21 consistent reference datasets for model validation of land surface fluxes and state  
22 (Seneviratne et al., 2010). The JJAS mean evapotranspiration from GLDAS, the IPSL and  
23 LMDZ model simulations are shown in Figs. 2(g-i) Note that the spatial distribution of the  
24 JJAS mean evapotranspiration from GLDAS (Fig. 2g) has resemblance with the pattern of  
25 observed monsoon precipitation (Fig. 2d). The regions of high evapotranspiration over  
26 central, west coast of India and along foot hills of Himalayas are better simulated in the high  
27 resolution LMDZ as compared to the IPSL model (Figs. 2h-i). It is noted that the pattern  
28 correlations of ET between the simulated and GLDAS dataset over the Indian land region  
29 ( $70^{\circ}$ - $90^{\circ}$ E,  $10^{\circ}$ - $28^{\circ}$ N) is 0.81 for LMDZ and 0.58 for the coarse resolution IPSL model. The  
30 better ET distribution in the high resolution LMDZ simulation, as compared to the IPSL  
31 coarse resolution model, is consistent with simulated precipitation in the two models. Note  
32 that the orographic precipitation along the west coast of India and foot hills of Himalayas are  
33 better captured in LMDZ, whereas the IPSL model significantly underestimates rainfall over



1 the Indian region resulting in low ET.

2 Here, we examine the annual water balance components at surface in terms of precipitation,  
3 evapotranspiration and runoff from the LMDZ and IPSL simulations and compare with the  
4 GLDAS dataset (Fig. 3). The Taylor diagram (Fig. 4; Taylor 2001) shows the skill of the  
5 models in simulating the annual spatial climatology and variability of precipitation, ET and  
6 runoff over the Indian land region with GLDAS as the reference dataset. The LMDZ model  
7 simulates the spatial pattern of precipitation relatively better than the IPSL model when  
8 compared to the GLDAS forcing (Fig. 4a). Although the LMDZ model overestimates the  
9 spatial variability in comparison with the coarser resolution GLDAS precipitation forcing and  
10 the CMAP observations, the magnitude is comparable with the high resolution gridded  
11 observational datasets (IMD and APHRODITE). The LMDZ model simulated spatial pattern  
12 and variability of evapotranspiration are closer to the estimates from the GLDAS multi-model  
13 mean as well as to each member models than that for the IPSL model (Fig. 4b). The total  
14 runoff simulated by the LMDZ model shows relatively better spatial pattern than the IPSL  
15 model in comparison with the GLDAS estimates (Fig. 4c). However this high resolution  
16 model overestimates the spatial variability relative to the coarser resolution GLDAS  
17 estimates. Additionally, it is important to ensure model simulations properly capture surface  
18 water balances on regional scales. Hasson et al. (2013) noted that biases in simulating annual  
19 surface water balances on regional scale often introduce considerable uncertainty in  
20 assessment of surface hydrological response to climate change. Keeping this in view, we  
21 examined the difference of annual precipitation minus evapotranspiration (P-ET) and the  
22 annual runoff averaged over the Indian land region (70.0°E-90.0°E; 10.0°N-28.0°N) from the  
23 GLDAS dataset and the two model simulations. The area-averaged values are shown in  
24 Table. 1. It can be noticed that the annual (P-ET) and runoff in GLDAS are in close balance  
25 (Table. 1). A reasonably good balance between (P-ET) and runoff can also be noted in the  
26 LMDZ simulation, whereas the annual runoff in the IPSL model far exceeds the (P-ET). The  
27 fairly consistent balance between the annual (P-ET) and runoff in the LMDZ model averaged  
28 over the Indian region provides confidence in interpreting the land surface hydrological  
29 variations as compared to the IPSL coarse resolution model.

### 30 **3.2 Simulation of climate trends over the monsoon region**

31 A climate model's credibility is increased if the model is able to simulate past variations in  
32 climate such as the trends over the twentieth century, when given realistic forcings (Flato et

1 al., 2013). The long-term drying trends (significant at > 95% level) in the summer monsoon  
2 precipitation over parts of central India, along the Indo Gangetic plains and the narrow  
3 western ghat region during the past half century from APHRODITE (Fig. 5a) are captured  
4 with higher magnitudes in the HIST simulation of LMDZ (Fig. 5c) model. While the driving  
5 IPSL model (Fig. 5b), shows significant increasing trends in precipitation over most parts of  
6 India. The observed (CRU) significant warming trends over most parts of India (Fig. 6a) are  
7 captured by both simulations, with relatively larger magnitude in LMDZ (Fig. 6c) than IPSL  
8 (Fig. 6b) model. Further detailed analysis based on the LMDZ model experiment with only  
9 natural forcing (NAT) brings out the role of anthropogenic forcing on these drying and  
10 warming trends over India. The observed (APHRODITE) rainfall shows a significant drying  
11 trend ( $-0.33 \text{ mm d}^{-1} (55 \text{ yr})^{-1}$ ) in summer monsoon precipitation over the Indian land region  
12 during 1951-2005 and the HIST simulations also shows a statistically significant trend of  $-0.8$   
13  $\text{mm d}^{-1} (55 \text{ yr})^{-1}$  (Fig. S4b). The observed (CRU) seasonal warming trend for the same  
14 period ( $0.5 \text{ }^{\circ}\text{C} (55\text{yr})^{-1}$ ) is significant over Indian land region and the HIST simulation of  
15 LMDZ model also captured a significant warming trend of  $1.1 \text{ }^{\circ}\text{C} (55\text{yr})^{-1}$  (Fig. S4a). The  
16 surface air temperature and precipitation trends simulated in response to natural forcings only  
17 (NAT) are generally close to zero, and inconsistent with observed trends over Indian land  
18 region. These findings are further supported by the simulated weaker summer monsoon  
19 circulation and reduced precipitation over Indian subcontinent in the HIST experiment of  
20 LMDZ model compared to the NAT experiment (Fig. S5). The finding that the observed  
21 changes are consistent with the LMDZ simulation that include human influence (HIST), and  
22 are inconsistent with that do not (NAT) would be sufficient for attribution studies as they  
23 typically assume that models simulate the large-scale spatial and temporal patterns of the  
24 response to external forcing correctly, but do not assume that models simulate the magnitude  
25 of the response correctly (Bindoff et al., 2013). Hence this high-resolution HIST simulation  
26 of LMDZ atmospheric model will be an important value addition for understanding the  
27 regional land surface hydrological responses that may be influenced by the anthropogenic  
28 forced changes in summer monsoon over the Indian subcontinent.

#### 29 **4 Response of land surface hydrology to the changing monsoon**

30 We further assess the long-term changes in the surface hydrologic variables such as soil  
31 moisture (SM) and ET in the HIST simulation of LMDZ. In association with the reduction of  
32 summer monsoon precipitation, the HIST simulation of LMDZ model also indicate

1 significant soil moisture (SM) drying trends over most parts of India (Fig. 7a). This accounts  
2 to about  $14 \text{ mm } (55 \text{ yr})^{-1}$  reduction in soil moisture (5%) when area averaged over the Indian  
3 land region. The comparison of the seasonal trends at each grid point over the Indian land  
4 region indicates a dominant control of precipitation on SM (Fig. S6). The SM is a source of  
5 water for the atmosphere through processes leading to ET from land, which include mainly  
6 plant transpiration and bare soil evaporation. The HIST simulation of LMDZ model show  
7 significant decrease of summer season mean ET over most parts of the Indian land region  
8 (Fig. 7b). The Indian land region area averaged reduction in ET accounts for about  $0.23 \text{ mm}$   
9  $\text{d}^{-1}(55\text{yr})^{-1}$  (9.5%). The simulated regions of ET reduction mostly coincide with that of drier  
10 soil moisture.

11 The global hydrological cycle is generally expected to intensify in a warming world, leading  
12 to increase in ET (Huntington, 2006). On the other hand, station observations of pan  
13 evaporation over India indicate a significant decreasing trend in recent decades  
14 (Padmakumari et al., 2013). Long-term trends in ET are basically driven by limiting factors  
15 such as soil moisture or radiation both on regional (Teuling et al., 2009) and global (Jung et  
16 al., 2010) scales. A comparison of the simulated seasonal ET trends at each grid point over  
17 Indian land region with the corresponding SM trends shows significant correlation between  
18 ET reduction and SM drying (Fig. 8a). This relationship is also noticed under conditions of  
19 increasing and decreasing surface incident solar radiation trends (Fig. 8b-c), implying that  
20 SM drying plays a dominant role in ET reduction over the Indian monsoon region, with  
21 minor contributions from changes in solar radiation reaching at surface. In fact, it can be  
22 noticed from Fig. 8b that decrease of ET is mostly accompanied by decrease of SM over a  
23 majority of grid-points over the Indian region, whereas increases in ET and global radiation  
24 are seen over fewer grid-points. The above analysis suggests that the SM drying trends,  
25 caused by local precipitation variations, largely drive ET reduction over the region.

## 26 **5 Future changes in surface hydrology**

27 The spatial distributions of the projected future trends in temperature, precipitation, soil  
28 moisture and evapotranspiration for the period 2006-2095 under RCP 4.5 scenario are shown  
29 in Fig. 9. The significant increase of temperature over the entire Indian land region is  
30 consistent with the increasing radiative effects of the rising CO<sub>2</sub> concentration in the future  
31 (Fig. 9a). The magnitude of this warming is larger (1.5 - 2 °C) at northern regions including  
32 Indo Gangetic planes and smaller along the western regions and the southern most parts of

1 India. The projected future trends in precipitation show regions of significant increase over  
2 western and south eastern parts and decrease over Central India (Fig. 9b). Note that the  
3 spatial pattern of trends in SM mostly follows the pattern of precipitation trends and is  
4 dominated by drying of SM (Fig. 9c). It is also interesting to note that the spatial pattern of  
5 projected trends in ET resembles the pattern of trends in SM (Fig. 9d).

6 The detectability of soil moisture changes to anthropogenic forcing is computed following the  
7 approach of Wetherald and Manabe (1999). The magnitudes of soil moisture changes with  
8 respect to the long term mean (1886-2005) of NAT integration are compared against the  
9 standard deviation of the natural soil moisture variability in the NAT integration. The changes  
10 are considered to be detectable when they exceed the standard deviation of the natural  
11 variability. For this analysis, we sequentially arrange variables for the HIST time period  
12 (1886-2005) and RCP4.5 scenario (2006-2095) as a continuous time-series, which will be  
13 henceforth referred to as ALL. Figure 10a shows the smoothed time-series of 20 year  
14 running-mean values of summer-monsoon soil moisture anomalies during 1886-2095 based  
15 on the high-resolution (LMDZ) and coarse-resolution (IPSL) simulations over the Central  
16 Indian region ( $74.5^{\circ}$ - $86.5^{\circ}$ E; $16.5^{\circ}$ - $26.5^{\circ}$ N; see box in Fig. 9a). The standard deviation of soil  
17 moisture in Fig. 10a is calculated from the corresponding natural (NAT) integrations. The  
18 appearance of a detectable change of soil moisture (exceeding one standard deviation of  
19 NAT) can be noted in the LMDZ simulation as early as 2010 and then the change is not  
20 prominent until 2050s and thereafter remains detectable till the end of 21st century. From Fig.  
21 10, one can note coherent evolution of the soil moisture and precipitation variations. In  
22 addition, we also see more persistence in detectability of soil moisture as compared to that of  
23 precipitation. This is consistent with the result that the soil moisture spectra is dominated by  
24 lower frequency variations as opposed to the precipitation spectra (see Delworth and Manabe,  
25 1988). On the other hand, the SM variations in the IPSL simulation show decadal-scale  
26 variations with slight decrease during latter part of the 21<sup>st</sup> century. Here, it is important to  
27 note that the surface warming trend during (1886-2005) is clearly borne out in both the IPSL  
28 and LMDZ models (Fig. 10b), with the magnitude of warming trend being more pronounced  
29 in the LMDZ simulation ( $0.21 \text{ K decade}^{-1}$ ) as compared to the IPSL model ( $0.15 \text{ K decade}^{-1}$ ).  
30 The appearance of a detectable change of soil moisture lags behind that of surface air  
31 temperature by several decades. This is due to the relatively smaller signal-to-noise ratio for  
32 soil moisture variability as compared to that of the surface air temperature (see Delworth and  
33 Manabe, 1989). Furthermore, the smaller signal-to-noise ratio of soil moisture over the

1 Indian region indicates relatively large natural interannual variability of summer monsoon  
2 precipitation (Fig. 10c). The IPSL model projection shows enhancement of monsoon  
3 precipitation and increase of soil moisture by the end of the 21<sup>st</sup> century (Figs. 10a, c). The  
4 decrease in monsoon precipitation over central India in the high-resolution LMDZ simulation  
5 is noticeable by early 21<sup>st</sup> century. It is also interesting to see that the high resolution  
6 simulation indicates decrease of soil moisture from middle to the end of 21<sup>st</sup> century over  
7 central India, despite a gradual revival of the projected monsoon precipitation by the mid 21<sup>st</sup>  
8 century. From the above discussion, it is seen that the high-resolution LMDZ simulations  
9 provide important value additions in terms of regional land surface response to changes in the  
10 South Asian monsoon.

## 11 **6 Conclusions**

12 We have used a state-of-the-art global climate model (LMDZ), with high-resolution  
13 telescopic zooming over South Asia, to investigate the regional land-surface response to  
14 changing climate and declining summer monsoon rains observed during the last few decades.  
15 This high-resolution climate model captures well the distribution of the mean monsoon  
16 rainfall and circulation features (Sabin et al., 2013). It is also noted that the high-resolution  
17 LMDZ model, which is coupled to a sophisticated land-surface parameterization scheme,  
18 displays a consistent surface water balance over the South Asian region - which is essential  
19 for making reliable assessments of the regional hydrological response to monsoonal changes.  
20 In the present work, we have performed two long-term simulation experiments, with and  
21 without anthropogenic forcing, for the historical period 1886-2005; and one future projection  
22 following the RCP4.5 scenario.

23 The results from our study suggest that the declining trend of monsoon precipitation over  
24 South Asia and weakening of large-scale summer monsoon circulation during the post-1950s  
25 are largely influenced by the anthropogenic forcing. It is found that the model simulated  
26 response to anthropogenic forcing shows an increase of surface temperature over the India  
27 region at a rate of  $1.1\text{ }^{\circ}\text{C}\text{ (55yr)}^{-1}$ , a decline of summer monsoon precipitation at a rate of  $0.8$   
28  $\text{mm d}^{-1}\text{ (55yr)}^{-1}$  and a corresponding reduction of soil moisture at a rate of  $14\text{ mm (55yr)}^{-1}$ .  
29 The simulated decrease of mean monsoon precipitation over the Indian region during the  
30 post-1950s is accompanied by a weakening of large-scale monsoon circulation and is  
31 consistent with observations (Krishnan et al. 2013). The results of a future climate projection  
32 using medium scenario (RCP 4.5) shows likely continuation of the drying trend in monsoon

1 rainfall and noticeable decrease of soil moisture till the end of the 21<sup>st</sup> century. The present  
2 high-resolution simulations are scientifically interesting, particularly given that only some of  
3 the CMIP5 models driven with same scenario generally show a decrease in mean  
4 precipitation over the Indian region, associated with large uncertainties (Chaturvedi et al.,  
5 2012).

6 The declining monsoonal rains and the associated hydro-climatic changes can have profound  
7 implications for crop production and socio-economic activities in the region. Our findings  
8 from the high-resolution LMDZ simulations suggest that persistent decrease of monsoon  
9 rainfall and soil moisture over the Indian region has significant impact on the regional land  
10 surface hydrology. The simulations show that a decrease of soil moisture over the Indian  
11 land region by 5% during 1951-2005 is accompanied by a decrease of ET by 9.5%. It is  
12 noticed that the ET reduction and SM drying, over the Indian land points, are significantly  
13 correlated even under conditions of increasing surface incident short wave radiation trends,  
14 implying that SM drying plays a dominant role in ET reduction in the region. While this  
15 study is based on a single realization, the realism of the high resolution simulation enhances  
16 our confidence in interpreting the land-surface hydrological response to climate change and  
17 declining monsoons. We realize that a suite of high resolution coupled model ensemble  
18 simulations will be required for attribution and quantifying uncertainties in the land surface  
19 hydrological response to monsoonal changes. This is a topic of future research and beyond  
20 the scope of the present study.

## 21 **Acknowledgements**

22 Authors thank Director IITM for extending all support for this research work. IITM is  
23 supported by Ministry of Earth Sciences, Government of India, New Delhi. The figures are  
24 prepared using GrADS. M. V. S. Ramarao is financially supported by the Indian Institute for  
25 Human Settlements (IIHS) through the Adaptation at Scale in Semi-Arid Regions (ASSAR)  
26 consortia of the Collaborative Adaptation Research initiative in Africa and Asia  
27 (CARIAA). This work is partially supported under the NORINDIA Project 216576/e10. We  
28 acknowledge the World Climate Research Programme's Working Group on Coupled  
29 Modeling, which is responsible for CMIP, and we thank the IPSL climate modeling group for  
30 producing and making available their model output.

31

## 1 **References**

- 2 Abish, B., Joseph, P. V. and Johannessen, O. M.: Weakening trend of the tropical easterly jet  
3 stream of the boreal summer monsoon season 1950-2009, *J. Clim.*, 26, 9408–9414,  
4 doi:10.1175/JCLI-D-13-00440.1, 2013.
- 5 Bindoff, N.L., Stott, P., AchutaRao, K., Allen, M., Gillett, N., Gutzler, D., Hansingo, K.,  
6 Hegerl, G., Hu, Y., Jain, S., Mokhov, I., Overland, J., Perlwitz, J., Sebbari, R., and Zhang, X.:  
7 Detection and Attribution of Climate Change: from Global to Regional, In: *Climate Change*  
8 2013: The Physical Science Basis. Contribution of Working Group I to the Fifth Assessment  
9 Report of the Intergovernmental Panel on Climate Change [Stocker, T.F., Qin, D., Plattner,  
10 G.-K., Tignor, M., Allen, S.K., Boschung, J., Nauels, A., Xia, Y., Bex, V. and Midgley,  
11 P.M. (eds.)], Cambridge University Press, Cambridge, United Kingdom and New York, NY,  
12 USA, 867–952, 2013.
- 13 Bollasina, M. A., Ming, Y. and Ramaswamy, V.: Anthropogenic Aerosols and the  
14 Weakening of the South Asian Summer Monsoon, *Science.*, 334(6055), 502–505,  
15 doi:10.1126/science.1204994, 2011.
- 16 Chaturvedi, R. K., Joshi, J., Jayaraman, M., Bala, G. and Ravindranath, N. H.: Multi-model  
17 climate change projections for India under representative concentration pathways, *Curr. Sci.*,  
18 103, 791–802, 2012.
- 19 Chung, C. E. and Ramanathan, V.: Weakening of north Indian SST gradients and the  
20 monsoon rainfall in India and the Sahel, *J. Clim.*, 19(2003), 2036–2045,  
21 doi:10.1175/JCLI3820.1, 2006.
- 22 Collins, M., AchutaRao, K., Ashok, K., Bhandari, S., Mitra, A. K., Prakash, S., Srivasatva,  
23 R. and Turner, A.: Observational challenges in evaluating climate models, *Nat. Clim.*  
24 *Change*, 3, 940–941, doi: 10.1038/nclimate2012, 2013.
- 25 Dee, D. P. and Uppala, S.: Variational bias correction of satellite radiance data in the ERA-  
26 Interim reanalysis, *Q. J. R. Meteorol. Soc.*, 135, 1830-1841, doi:10.1002/qj.493, 2009.
- 27 Dee, D. P., Uppala, S. M., Simmons, A. J., Berrisford, P., Poli, P., Kobayashi, S., Andrae, U.,  
28 Balmaseda, M. A., Balsamo, G., Bauer, P., Bechtold, P., Beljaars, A. C. M., van de Berg, L.,  
29 Bidlot, J., Bormann, N., Delsol, C., Dragani, R., Fuentes, M., Geer, A. J., Haimberger, L.,

1 Healy, S. B., Hersbach, H., Hólm, E. V., Isaksen, L., Kållberg, P., Köhler, M., Matricardi,  
2 M., McNally, A. P., Monge-Sanz, B. M., Morcrette, J.-J., Park, B.-K., Peubey, C., de Rosnay,  
3 P., Tavolato, C., Thépaut, J.-N. and Vitart, F.: The ERA-Interim reanalysis: configuration and  
4 performance of the data assimilation system, *Q. J. R. Meteorol. Soc.*, 137: 553–597. doi:  
5 10.1002/qj.828, 2011.

6 Delworth, T. L. and Manabe, S.: The influence of potential evaporation on the variabilities of  
7 simulated soil wetness and climate, *J. Clim.*, 1, 523–547, 1988.

8 Delworth, T. L. and Manabe, S.: The Influence of soil wetness on near-surface atmospheric  
9 variability, *J. Clim.*, 2, 1447–1462, 1989.

10 De Rosnay, P. and Polcher, J.: Modelling root water uptake in a complex land surface scheme  
11 coupled to a GCM, *Hydrol. Earth Syst. Sci.*, 2, 239–255, doi:10.5194/hess-2-239-1998, 1998.

12 Ducoudré, N. I., Laval, K. and Perrier, A.: SECHIBA, a New Set of Parameterizations of the  
13 Hydrologic Exchanges at the Land-Atmosphere Interface within the LMD Atmospheric  
14 General Circulation Model, *J. Clim.*, 6, 248–273, doi:10.1175/1520-  
15 0442(1993)006<0248:SANSOP>2.0.CO;2, 1993.

16 Dufresne, J.-L., Foujols, M.-A., Denvil, S., Caubel, A., Marti, O., Aumont, O.,  
17 Balkanski, Y., Bekki, S., Bellenger, H., Benschila, R., Bony, S., Bopp, L., Braconnot,  
18 P., Brockmann, P., Cadule, P., Cheruy, F., Codron, F., Cozic, A., Cugnet, D., de  
19 Noblet, N., Duvel, J.-P., Ethé, C., Fairhead, L., Fichefet, T., Flavoni, S., Friedlingstein,  
20 P., Grandpeix, J.-Y., Guez, L., Guilyardi, E., Hauglustaine, D., Hourdin, F., Idelkadi, A.,  
21 Ghattas, J., Joussaume, S., Kageyama, M., Krinner, G., Labetoulle, S., Lahellec, A.,  
22 Lefebvre, M.-P., Lefevre, F., Levy, C., Li, Z. X., Lloyd, J., Lott, F., Madec, G., Mancip,  
23 M., Marchand, M., Masson, S., Meurdesoif, Y., Mignot, J., Musat, I., Parouty, S.,  
24 Polcher, J., Rio, C., Schulz, M., Swingedouw, D., Szopa, S., Talandier, C., Terray, P.,  
25 Viovy, N. and Vuichard, N. : Climate change projections using the IPSL-CM5 Earth System  
26 Model: from CMIP3 to CMIP5, *Climate Dynam.*, 40, 2123–2165,doi:10.1007/s00382-012-  
27 1636-1, 2013.

28 Douville, H., Royer, J.-F., Polcher, J., Cox, P., Gedney, N., Stephenson, D.B. and Valdes,  
29 P.J.: Impact of doubling CO<sub>2</sub> on the Asian summer monsoon: robust versus model-dependent  
30 responses, *J. Meteorol. Soc. Jap.*, 78,421–439, 2000.



1 Fan, F., Mann, M. E., Lee, S. and Evans, J. L.: Observed and modeled changes in the South  
2 Asian summer monsoon over the historical period, *J. Clim.*, 23, 5193–5205,  
3 doi:10.1175/2010JCLI3374.1, 2010.

4 Flato, G., Marotzke, J., Abiodun, B., Braconnot, P., Chou, S.C., Collins, W., Cox, P.,  
5 Driouech, F., Emori, S., Eyring, V., Forest, C., Gleckler, P., Guilyardi, E., Jakob, C., Kattsov,  
6 V., Reason C., and Rummukainen, M. : Evaluation of Climate Models. In: *Climate Change*  
7 *2013: The Physical Science Basis. Contribution of Working Group I to the Fifth Assessment*  
8 *Report of the Intergovernmental Panel on Climate Change [Stocker, T.F., Qin, D., Plattner,*  
9 *G.-K., Tignor, M., Allen, S.K., Boschung, J., Nauels, A., Xia, Y., Bex, V. and Midgley,*  
10 *P.M. (eds.)]. Cambridge University Press, Cambridge, United Kingdom and New York, NY,*  
11 *USA, 741–866, doi:10.1017/CBO9781107415324.020, 2013.*

12 Guhathakurta, P., Rajeevan, M.: Trends in the rainfall pattern over India, National climate  
13 Centre (NCC) Research Report No.2, 1–23, India. Met. Department., Pune, 2006.

14 Harris, I., Jones. P. D., Osborn, T. J. and Lister, D. H.: Updated high-resolution grids of  
15 monthly climatic observations – the CRU TS3.10 Dataset, *Int. J. Climatol.*, 34, 623–642, doi:  
16 10.1002/joc.3711, 2014.

17 Hasson, S., Lucarini, V. and Pascale, S.: Hydrological cycle over South and Southeast Asian  
18 river basins as simulated by PCMDI/CMIP3 experiments, *Earth Syst. Dyn.*, 4, 199–217,  
19 doi:10.5194/esd-4-199-2013, 2013.

20 Hourdin, F., Musat, I., Bony, S., Braconnot, P., Codron, F., Dufresne, J. L., Fairhead, L.,  
21 Filiberti, M. A., Friedlingstein, P., Grandpeix, J. Y., Krinner, G., LeVan, P., Li, Z. X. and  
22 Lott, F.: The LMDZ4 general circulation model: Climate performance and sensitivity to  
23 parametrized physics with emphasis on tropical convection, *Clim. Dyn.*, 27, 787–813,  
24 doi:10.1007/s00382-006-0158-0, 2006.

25 Huntington, T. G.: Evidence for intensification of the global water cycle: Review and  
26 synthesis, *J. Hydrol.*, 319, 83–95, 2006.

27 Hurtt, G., Chini, L., Frolking, S., Betts, R., Feddema, J., Fischer, G., Fisk, J., Hibbard, K.,  
28 Houghton, R., Janetos, A., Jones, C., Kindermann, G., Kinoshita, T., Klein Goldewijk, K.,  
29 Riahi, K., Shevliakova, E., Smith, S., Stehfest, E., Thomson, A., Thornton, P., van Vuuren,

1 D. and Wang, Y.: Harmonization of land-use scenarios for the period 1500–2100: 600 years  
2 of global gridded annual land-use transitions, wood harvest, and resulting secondary lands.  
3 *Climatic Change*, 109, 117–161, doi:10.1007/s10584-011-0153-2, 2011.

4 Jourdain, N. C., Gupta, A. Sen, Taschetto, A. S., Ummenhofer, C. C., Moise, A. F. and  
5 Ashok, K.: The Indo-Australian monsoon and its relationship to ENSO and IOD in reanalysis  
6 data and the CMIP3/CMIP5 simulations, *Clim. Dyn.*, 41, 3073–3102, doi:10.1007/s00382-  
7 013-1676-1, 2013.

8 Jung, M., Reichstein, M., Ciais, P., Seneviratne, S. I., Sheffield, J., Goulden, M. L., Bonan,  
9 G., Cescatti, A., Chen, J., de Jeu, R., Dolman, a J., Eugster, W., Gerten, D., Gianelle, D.,  
10 Gobron, N., Heinke, J., Kimball, J., Law, B. E., Montagnani, L., Mu, Q., Mueller, B., Oleson,  
11 K., Papale, D., Richardson, A. D., Rouspard, O., Running, S., Tomelleri, E., Viovy, N.,  
12 Weber, U., Williams, C., Wood, E., Zaehle, S. and Zhang, K.: Recent decline in the global  
13 land evapotranspiration trend due to limited moisture supply., *Nature*, 467, 951–954,  
14 doi:10.1038/nature09396, 2010.

15 Kim, J., Sanjay, J., Mattmann, C., Boustani, M., Ramarao, M. V. S., Krishnan, R. and  
16 Waliser, D.: Uncertainties in estimating spatial and interannual variations in precipitation  
17 climatology in the India–Tibet region from multiple gridded precipitation datasets, *Int. J.*  
18 *Climatol.*, doi: 10.1002/joc.4306, 2015.

19 Kitoh, A., Yukimoto, S., Noda, A. and Motoi, T.: Simulated changes in the Asian summer  
20 monsoon at times of increased atmospheric CO<sub>2</sub>, *J. Met. Soc. Jap*, 75, 1019–1031, 1997.

21 Krinner, G., Viovy, N., de Noblet-Ducoudré, N., Oge´e, J., Polcher, J., Friedlingstein, P.,  
22 Ciais, P., Sitch, S. and Prentice, C.: A dynamic global vegetation model for studies of the  
23 coupled atmosphere-biosphere system, *Glob. Biogeochem. cycles*, 19, GB1015,  
24 doi:10.1029/2003GB002199, 2005.

25 Krishnan, R., Sabin, T. P., Ayantika, D. C., Kitoh, A., Sugi, M., Murakami, H., Turner, A.  
26 G., Slingo, J. M. and Rajendran, K.: Will the South Asian monsoon overturning circulation  
27 stabilize any further?, *Clim. Dyn.*, 40, 187–211, doi:10.1007/s00382-012-1317-0, 2013.

- 1 Kumar, K. N., Rajeevan, M., Pai, D. S., Srivastava, A. K. and Preethi, B.: On the observed  
2 variability of monsoon droughts over India, *Weather Clim. Extrem.*, 1, 42–50,  
3 doi:10.1016/j.wace.2013.07.006, 2013.
- 4 Loveland, T.R., Reed, B.C., Brown, J.F., Ohlen, D.O., Zhu, Z., Yang, L. and Merchant, J.W.:  
5 Development of a global land cover characteristics database and IGBP DISCover from 1 km  
6 AVHRR data, *Int. J. Remote. Sens.*, 21(6–7), 1303–1330, doi:10.1080/014311600210191,  
7 2000.
- 8 Maraun, D.: (2012) Nonstationarities of regional climate model biases in European seasonal  
9 mean temperature and precipitation sums, *Geophys. Res. Lett.*, 39,L06706, 2012.
- 10 Padmakumari, B., Jaswal, A. K. and Goswami, B. N.: Decrease in evaporation over the  
11 Indian monsoon region: Implication on regional hydrological cycle, *Clim. Change*, 121, 787–  
12 799, doi:10.1007/s10584-013-0957-3, 2013.
- 13 Pai, D. S., Sridhar Latha, Rajeevan, M., Sreejith, O. P., Satbhai, N. S., Mukhopadhyay, B.:  
14 Development of a new high spatial resolution ( $0.25^\circ \times 0.25^\circ$ ) long period (1901–2010) daily  
15 gridded rainfall data set over India and its comparison with existing data sets over the region,  
16 *Mausam*, 65, 1–18, 2014.
- 17 Rajendran, K., Kitoh, A., Srinivasan, J., Mizuta, R. and Krishnan, R.: Monsoon circulation  
18 interaction with Western Ghats orography under changing climate projection by a 20-km  
19 mesh AGCM, *Theor. Appl. Climatol.*, 110, 555–571, doi: 10.1007/s00704-012-0690-2,  
20 2012.
- 21 Rodell, M., Houser, P.R., Jambor, U., Gottschalck, J., Mitchell, K., Meng, C-J., Arsenault,  
22 K., Cosgrove, B., Radakovich, J., Bosilovich, M., Entin, J. K., Walker, J. P., Lohmann, D.  
23 and Toll, D.: The Global Land Data Assimilation System, *Bull. Am. Meteorol. Soc.*, 85, 381-  
24 394, 2004.
- 25 Sabin, T. P., Krishnan, R., Ghattas, J., Denvil, S., Dufresne, J. L., Hourdin, F. and Pascal, T.:  
26 High resolution simulation of the South Asian monsoon using a variable resolution global  
27 climate model, *Clim. Dyn.*, 41, 173–194, doi:10.1007/s00382-012-1658-8, 2013.

- 1 Sadourny, R. and Laval, K.: January and July performance of the LMD general circulation  
2 model, In: Berger A, Nicolis C (eds) *New perspectives in climate modeling*, Elsevier,  
3 Amsterdam, pp 173–197, 1984.
- 4 Saha, A., Ghosh, S., Sahana, A. S., and Rao, E. P.: Failure of CMIP5 climate models in  
5 simulating post-1950 decreasing trend of Indian monsoon, *Geophys. Res. Lett.*, 41, 7323–  
6 7330, doi:10.1002/2014GL061573, 2014.
- 7 Seneviratne, S. I., Corti, T., Davin, E. L., Hirschi, M., Jaeger, E. B., Lehner, I., Orlowsky, B.  
8 and Teuling, A. J.: Investigating soil moisture-climate interactions in a changing climate: A  
9 review, *Earth-Science Rev.*, 99(3-4), 125–161, doi:10.1016/j.earscirev.2010.02.004, 2010.
- 10 Seneviratne, S. I., Lüthi, D., Litschi, M. and Schär, C.: Land-atmosphere coupling and  
11 climate change in Europe., *Nature*, 443, 205–209, doi:10.1038/nature05095, 2006.
- 12 Seneviratne, S. I., Pal, J. S., Eltahir, E. A. B. and Schär, C.: Summer dryness in a warmer  
13 climate: A process study with a regional climate model, *Clim. Dyn.*, 20, 69–85,  
14 doi:10.1007/s00382-002-0258-4, 2002.
- 15 Singh, D., Tsiang, M., Rajaratnam, B. and Diffenbaugh, N. S.: Observed changes in extreme  
16 wet and dry spells during the South Asian summer monsoon season, *Nat. Clim. Chang.*, 4, 1–  
17 6, doi:10.1038/nclimate2208, 2014.
- 18 Tanaka, H.L., Ishizaki, N. and Kitoh, A.: Trend and interannual variability of Walker,  
19 monsoon and Hadley circulations defined by velocity potential in the upper troposphere,  
20 *Tellus*, 56A, 250–269, 2004.
- 21 Taylor, K.E.: Summarizing multiple aspects of model performance in a single diagram, *J.*  
22 *Geo. Res.*, 106, 7183–7192, doi:10.1029/2000JD900719, 2001.
- 23 Taylor, K. E., Stouffer, R. J. and Meehl, G. a.: An overview of CMIP5 and the experiment  
24 design, *Bull. Am. Meteorol. Soc.*, 93, 485–498, doi:10.1175/BAMS-D-11-00094.1, 2012.
- 25 Teuling, A. J., Hirschi, M., Ohmura, A., Wild, M., Reichstein, M., Ciais, P., Buchmann, N.,  
26 Ammann, C., Montagnani, L., Richardson, A. D., Wohlfahrt, G. and Seneviratne, S. I.: A  
27 regional perspective on trends in continental evaporation, *Geophys. Res. Lett.*, 36, 1–5,  
28 doi:10.1029/2008GL036584, 2009.

1 Ueda, H., Iwai, A., Kuwako, K. and Hori, M. E.: Impact of anthropogenic forcing on the  
2 Asian summer monsoon as simulated by eight GCMs, *Geophys. Res. Lett.*, 33, L06703,  
3 doi:10.1029/2005GL025336, 2006.

4 Veechi, G. A., Soden, B. J., Wittenberg, A. T., Held, I. M., Leetma, A. and Harrison, M. J.:  
5 Weakening of tropical Pacific atmospheric circulation due to anthropogenic forcing, *Nature*,  
6 441, 73–76, 2006.

7 Wetherald, R.T. and Manabe, S.: Detectability of summer dryness caused by greenhouse  
8 warming, *Clim. Change.*, 43, 495-511, 1999.

9 Xie, P. and Arkin, P. A.: Global precipitation: A 17-year monthly analysis based on gauge  
10 observations, satellite estimates, and numerical model outputs, *Bull. Am. Meteorol. Soc.*, 78,  
11 2539 - 2558, 1997.

12 Yatagai, A., Kamiguchi, K., Arakawa, O., Hamada, A., Yasutomi, N. and Kitoh, A.:  
13 APHRODITE: Constructing a long-term daily gridded precipitation dataset for Asia based  
14 on a dense network of rain gauges, *Bull. Am. Met. Soc.*, 93, 1401- 1415,  
15 doi:10.1175/BAMS-D-11-00122.1, 2012.

16  
17  
18  
19  
20  
21  
22  
23  
24  
25  
26  
27  
28  
29  
30  
31

1 **Table 1.** Long term annual means in mm d<sup>-1</sup> for precipitation (P), Evapotranspiration (ET),  
 2 runoff (R) and P-ET from GLDAS, IPSL and LMDZ models during 1979-2005 averaged  
 3 over the domain 70°-90°E;10°-28°N. The water balance is highlighted.

	<b>GLDAS</b>	<b>IPSL</b>	<b>LMDZ</b>
P	2.63	1.81	2.97
ET	1.99	2.25	1.92
R	<b>0.65</b>	<b>0.28</b>	<b>1.06</b>
P-ET	<b>0.64</b>	<b>-0.44</b>	<b>1.05</b>

4  
5  
6  
7  
8  
9  
10  
11  
12  
13  
14  
15  
16  
17  
18  
19  
20  
21  
22  
23  
24  
25  
26  
27  
28

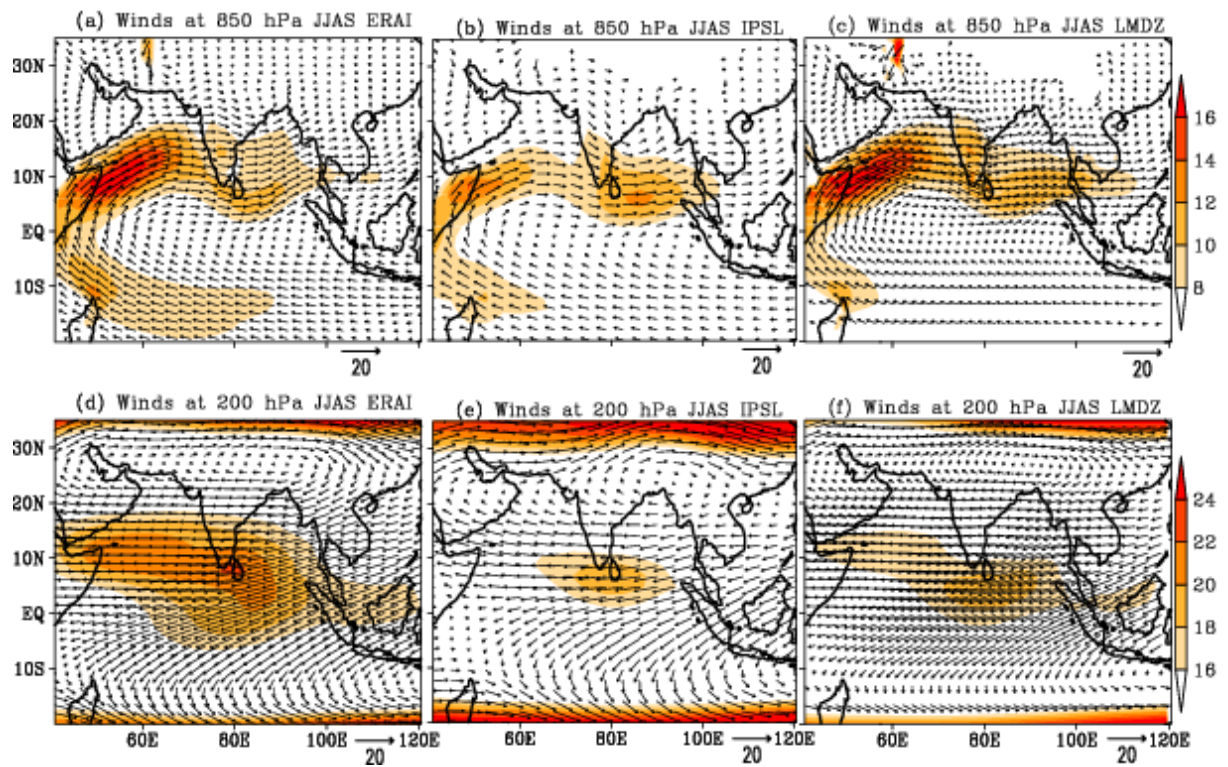


Figure 1. Spatial maps for JJAS mean wind fields ( $\text{m s}^{-1}$ ) at (top) 850 hPa and (bottom) 200hPa for (a,d) ERAI (1979-2005), (b,e) IPSL (1951-2005) and (c,f) LMDZ (1951-2005) simulations. Shading denotes wind magnitude.

- 1
- 2
- 3
- 4
- 5
- 6
- 7
- 8

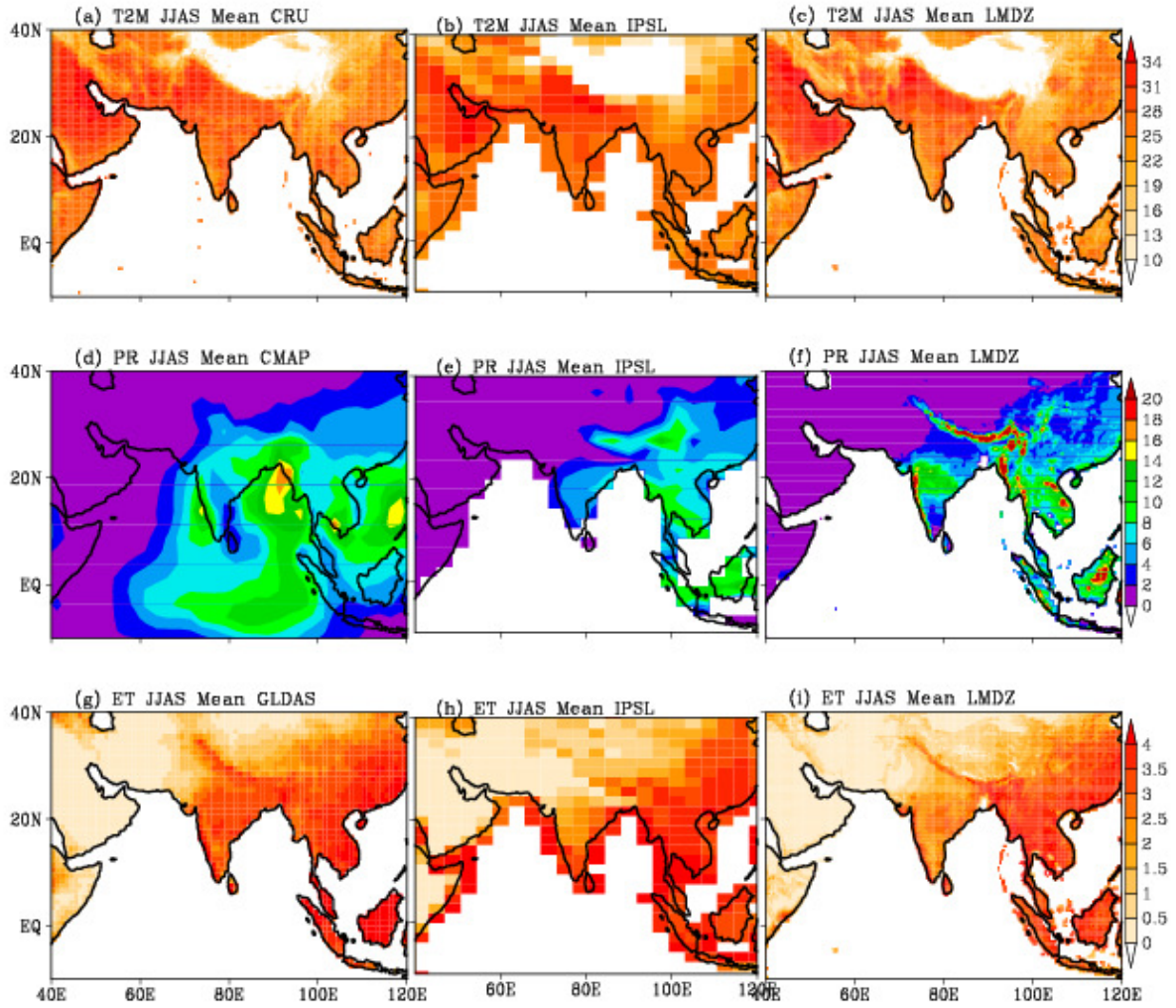


Figure 2. Spatial distributions of JJAS mean (top) 2m air temperature (T2M; °C), (middle) precipitation (PR; mm d<sup>-1</sup>) and (bottom) evapotranspiration (ET; mm d<sup>-1</sup>) from (a,d,g) observations/multi model data, from HIST simulations of (b,e,h) IPSL and (c,f,i) LMDZ models . The period of analysis for CMAP and GLDAS is 1979-2005 and for CRU, model simulations the time period is 1951-2005.

- 1
- 2
- 3
- 4
- 5
- 6
- 7
- 8



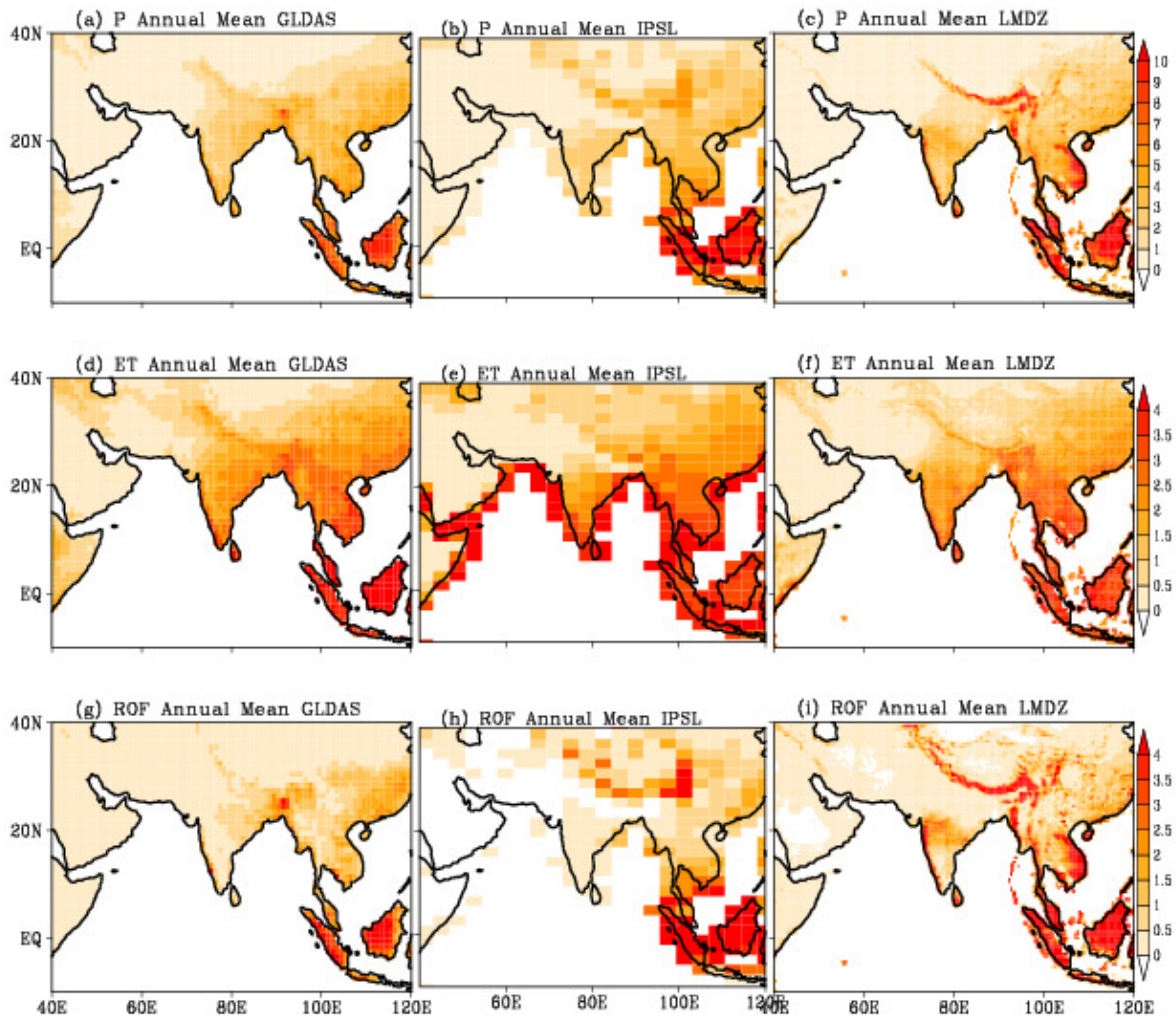
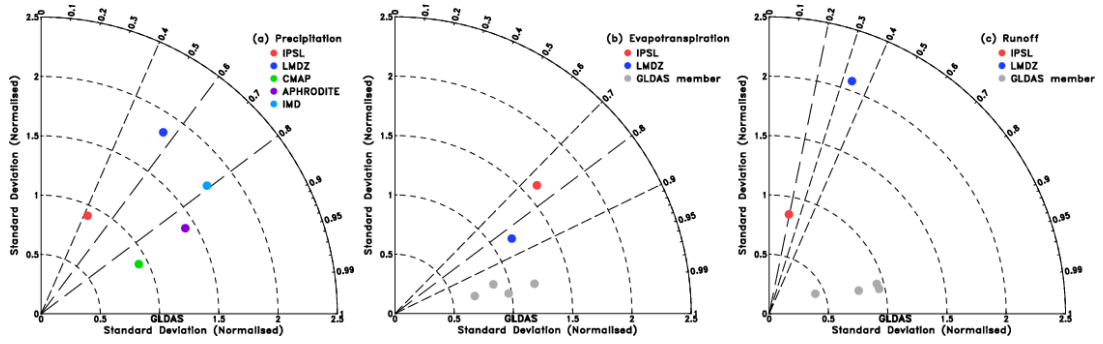


Figure 3. Spatial maps for annual mean (top) precipitation, (middle) evapotranspiration and (bottom) runoff from (a,d,g)GLDAS, (b,e,h)IPSL and (c,f,i)LMDZ simulations during 1979-2005. Units are  $\text{mm d}^{-1}$ .



**Figure 4.** Taylor diagram for the annual-mean (a) precipitation, (b) evapotranspiration and (c) total runoff climatology (1979-2005) from the IPSL and LMDZ model simulations averaged over land grid points in India ( $70^{\circ}\text{E}$ - $90^{\circ}\text{E}$ ;  $10^{\circ}\text{N}$ - $28^{\circ}\text{N}$ ). The radial coordinate shows the standard deviation of the spatial pattern, normalized by the observed standard deviation. The azimuthal variable shows the correlation of the modelled spatial pattern with the observed spatial pattern. The distance between the reference dataset (GLDAS) and individual points corresponds to root mean square error (RMSE).

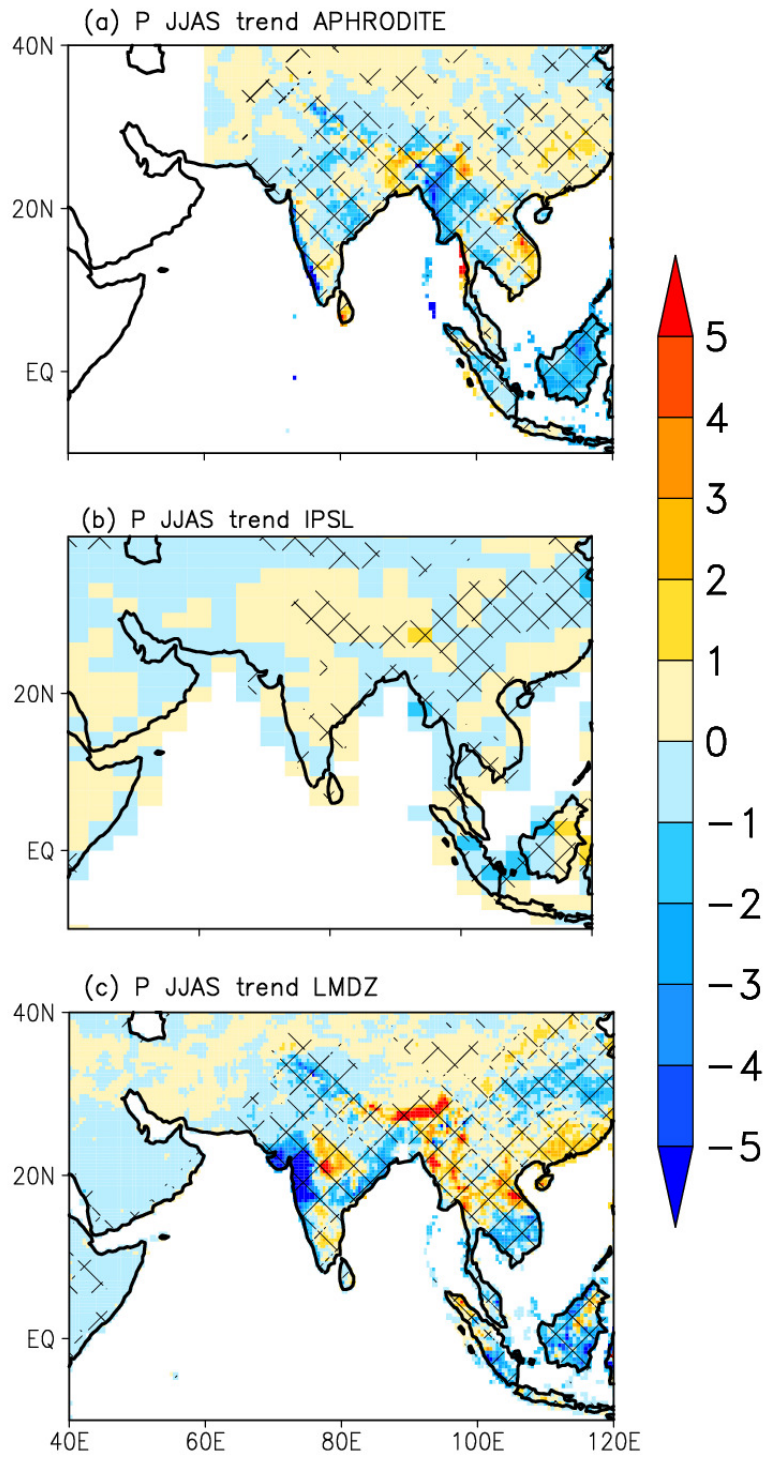


Figure 5. Spatial maps of linear trends in JJAS rainfall based on (a) APHRODITE, (b) IPSL and (c) LMDZ HIST simulation. Units are  $\text{mm d}^{-1}$  change over the period 1951–2005. Trend values exceeding the 95% level of statistical significance based on Students  $t$  test are hatched.

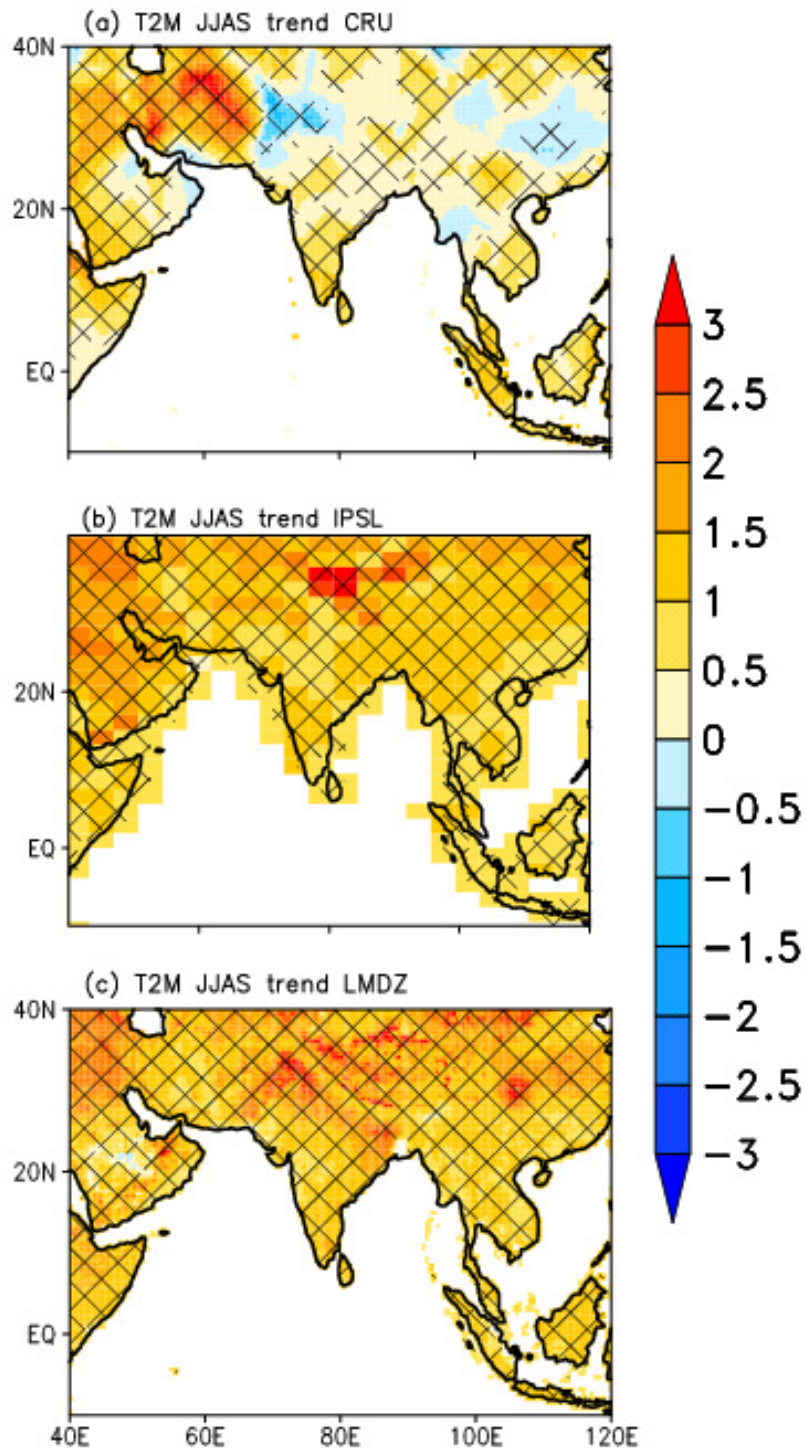


Figure 6. Spatial maps of linear trends in 2m air temperature for JJAS season based on (a) CRU, (b) IPSL and (c) LMDZ HIST simulation. Units are  $^{\circ}\text{C}$  change over the period 1951–2005. Trend values exceeding the 95% level of statistical significance based on Students t test are hatched.

1

2



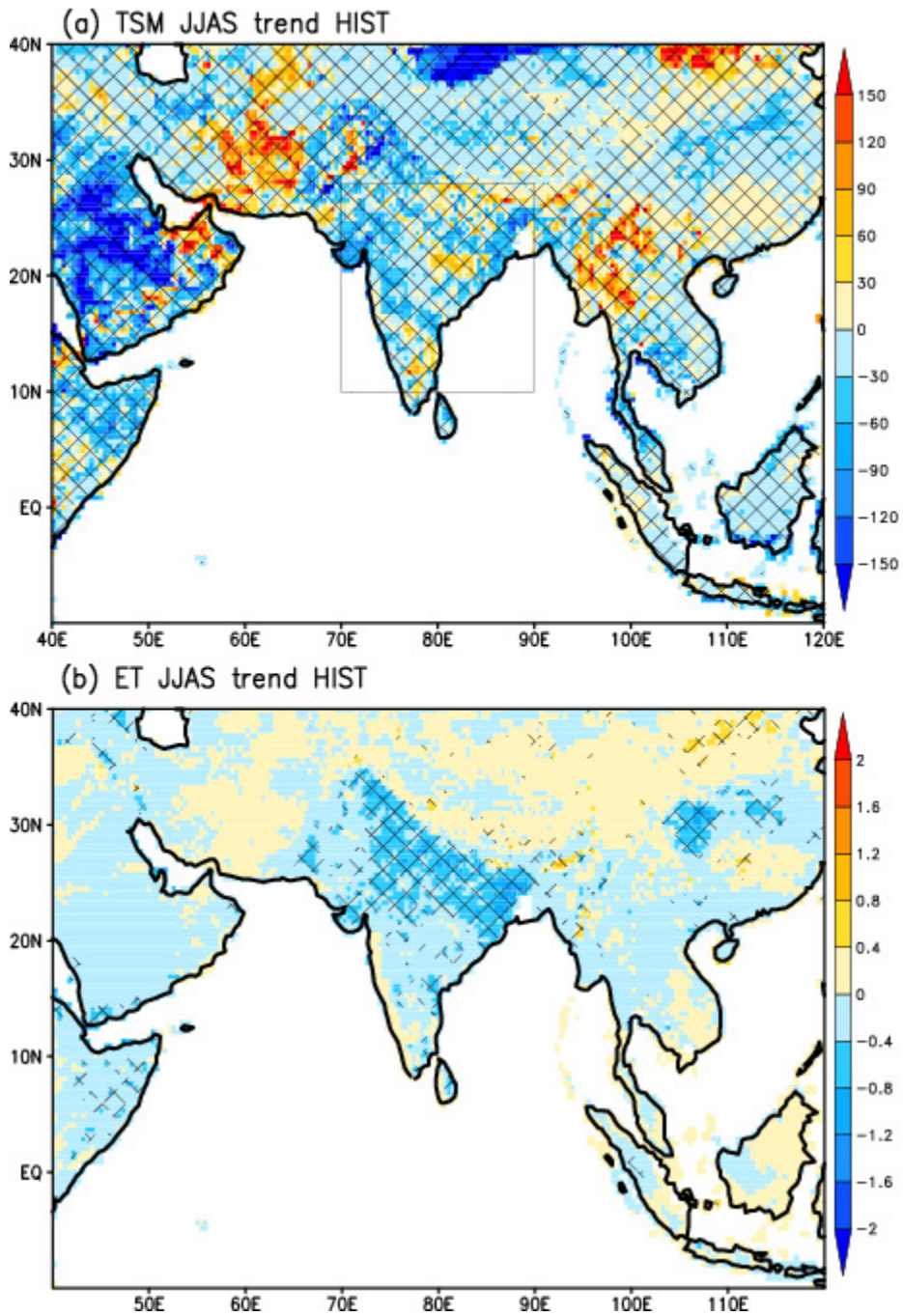
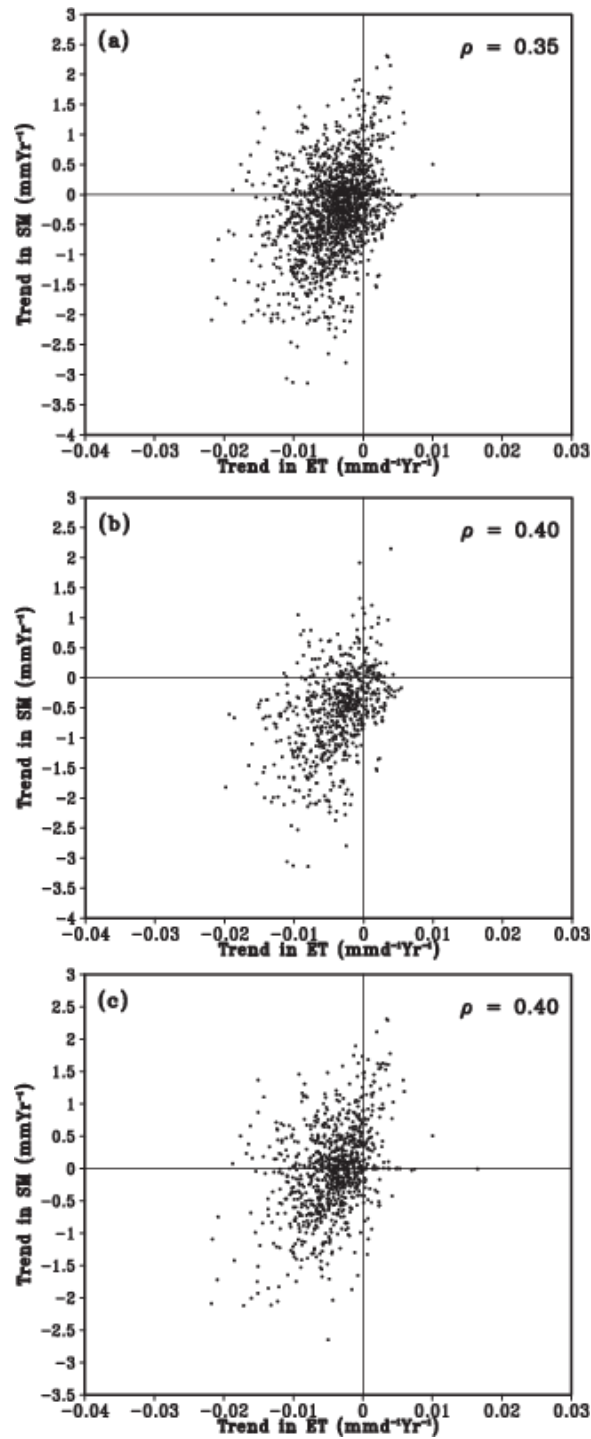


Figure 7. Spatial distribution of linear trends in JJAS mean (a) total soil moisture (SM) and evapotranspiration (ET) from HIST simulation of LMDZ. Units are mm and  $\text{mm d}^{-1}$  change over the period 1951–2005 for SM and ET respectively. Trend values exceeding the 95% level of statistical significance based on Students t test are hatched.

- 1
- 2
- 3



**Figure 8.** (a) Scatter plot of linear trends in JJAS mean evapotranspiration(ET) during the 55-year (1951-2005) period as a function of the linear trends of total soil moisture(SM) for all the grid points over the region 70°E-90°E; 10°N-28°N. (b and c) same as (a) expect for the grid points with trends in surface downward short wave radiation (b) increasing and (c)decreasing.

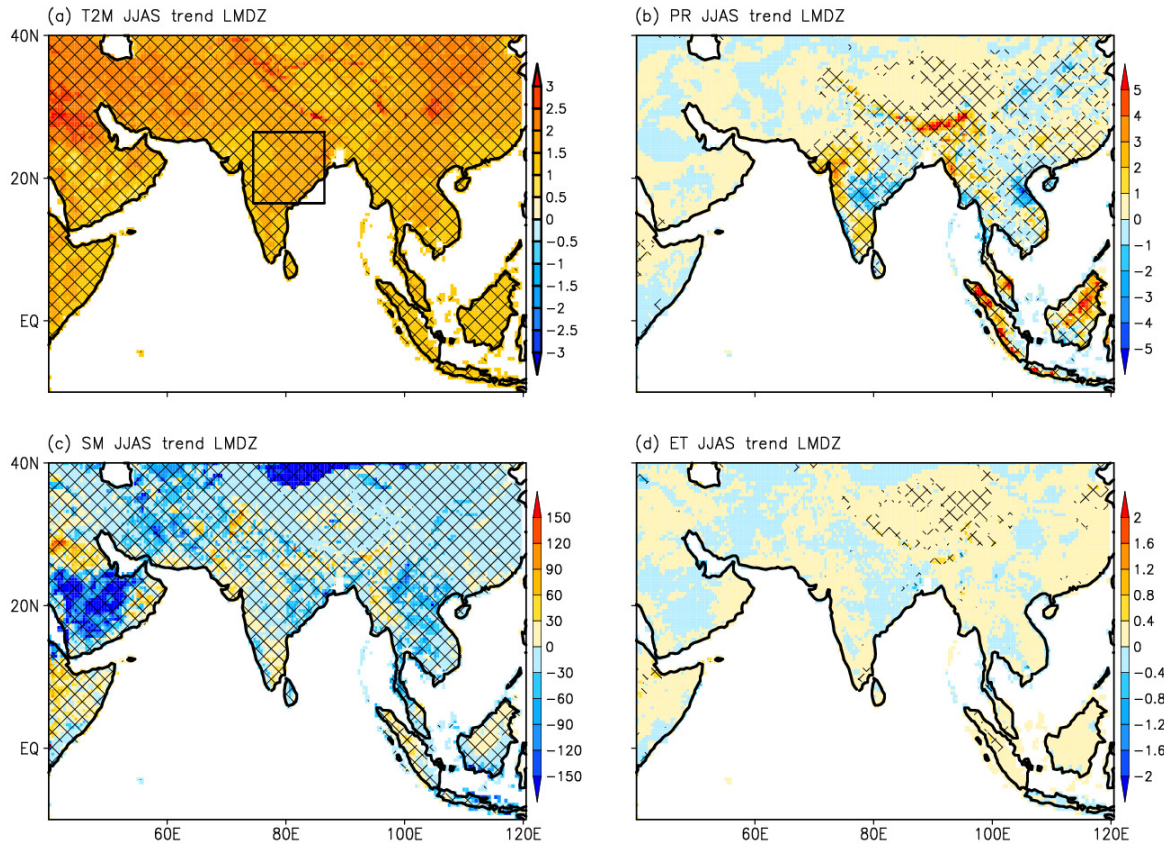


Figure 9. Spatial distribution of linear trends in (a) 2m air temperature ( $^{\circ}\text{C}$ ), (b) precipitation ( $\text{mm d}^{-1}$ ), (c) soil moisture ( $\text{mm}$ ) and (d) evapotranspiration ( $\text{mm d}^{-1}$ ) from RCP simulation of LMDZ. Trends are expressed as change over the period 2006–2095. Trend values exceeding the 95% level of statistical significance based on Students  $t$  test are hatched. The box indicates central India ( $74.5^{\circ}$ - $86.5^{\circ}\text{E}$ ; $16.5^{\circ}$ - $26.5^{\circ}\text{N}$ ) region.

1

2

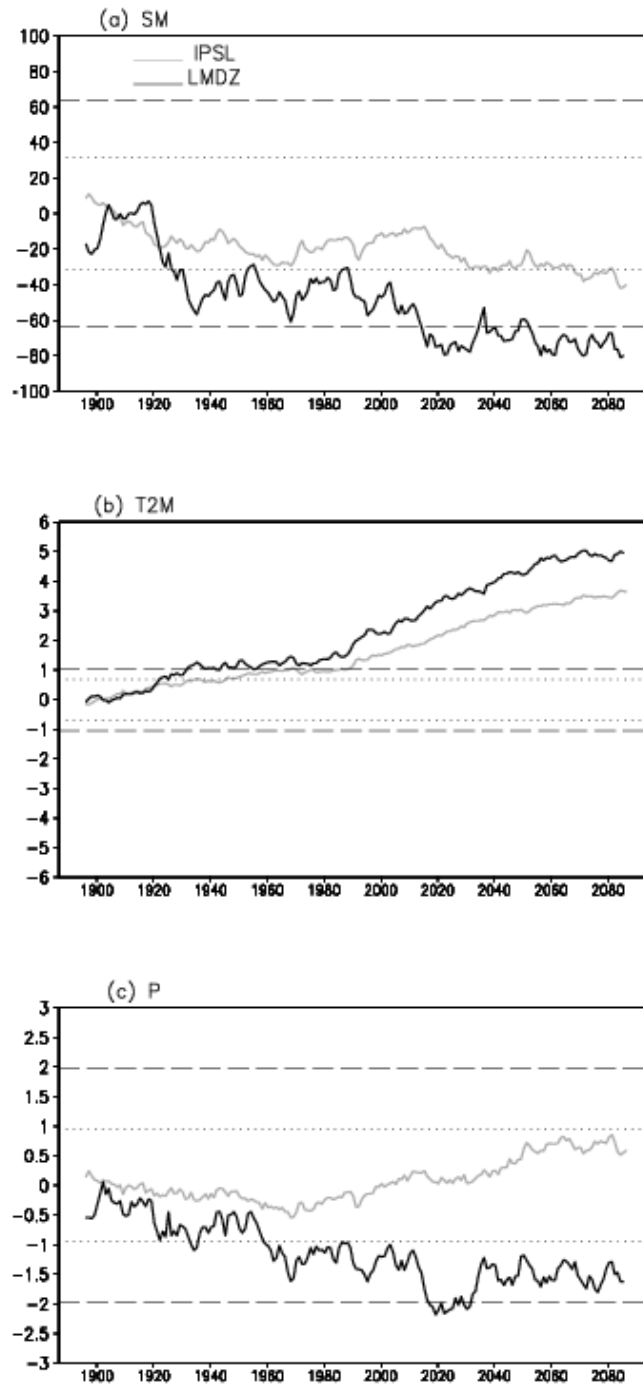


Figure 10. Time series of area-averaged anomalies of (a) soil moisture (SM; mm), (b) 2m air temperature (T2M; °C) and (c) Precipitation (P; mm d<sup>-1</sup>) from ALL (HIST and RCP) experiments of (grey) IPSL and (black) LMDZ for the region 74.5°-86.5°E;16.5°-26.5°N. The yearly JJAS anomalies are computed as the difference from the corresponding long-term mean (1886-2005) of NAT integration. Each time series has been smoothed by a 20 year running mean. The two horizontal dashed lines denote one standard deviation limits from the NAT integration computed from the yearly JJAS averages for LMDZ and dotted lines correspond to IPSL.